2022 IEEE International Conference on Electronics, Computing and Communication Technologies (CONECCT) | 978-1-6654-9781-7/22/$31.00 ©2022 IEEE | DOI: 10.1109/CONECCT55679.2022.9865747

Comb-Shaped Patch Antenna Design Study with Shifted Arms and Asymmetric Architecture Enabling Controlled Resonance Change and Radiation Pattern

Melih Aslan
Electrical and Electronics Engineering Department
Abdullah Gul University
Kayseri, Turkey
melih.aslan@agu.edu.tr

Huseyin Baydar
Electrical and Electronics Engineering Department
Abdullah Gul University
Kayseri, Turkey
huseyin.baydar@agu.edu.tr

Veli Tayfun Kilic
Electrical and Electronics Engineering Department
Abdullah Gul University
Kayseri, Turkey
tayfun.kilic@agu.edu.tr

***Abstract*—This paper reports comb-shaped patch antennas with asymmetrical geometries having two and three arms on the sides. The proposed geometry is evolved from regular rectangular shaped patch antenna by removing certain parts of the radiator patch and shifting the arms on one side of the antenna. Systematic simulations were obtained with the designed antennas for different arm shifting distances, and changes in resonance behavior and far-field radiation pattern were investigated. Results show that as the arm shifting increases the first and second resonance frequencies of the antennas decrease. Also, it is observed that the radiation occurs with two symmetric beams at the second resonance frequency of the designed antennas with no shift between the arms. However, as the arm shifting is applied the beam on the side of the arms closer to the feeding line gets stronger, whereas the other beam weakens. Obtained plots indicate that the directivity of the antennas have a tendency to increase with the arm shifting while the side lobe level decreases. In addition, results show that the half power beam width of the antenna increases with arm shifting. The simulations were repeated for different arm thicknesses and the same observations were held.**

Keywords—patch antenna, comb-shaped, radiation pattern

I. Introduction

Antennas are devices that capture electromagnetic waves propagating in space and transmit them to a transmission line or vice versa [1]. Since antennas have wide usage of areas, they come in many different structures and features depending on the application [2]. Also, depending on their radiation antennas can be classified into three main categories that are isotropic, omnidirectional and directional antennas [3]. Isotropic antennas radiate electromagnetic power equally in all directions in three-dimensional (3D) space. Point sources are considered as isotropic antennas. Although point sources do not actually exist, isotropic antennas are important in analysis and while making comparisons [1]. Monopole and dipole antennas, on the other hand, are examples of omnidirectional antennas, radiating in a plane with equal power in all directions [4]. Such antennas are generally used to capture signals from all directions on a plane in applications that do not have a fixed transceiver location, such as portable FM-AM receivers, walkie-talkies, and some mobile phones [5]. Moreover, Yagi-Uda antennas, dish antennas, horn antennas, and microstrip patch antennas are examples of directional antennas [6]. These antennas generally have different operating frequencies and they are used in distinct applications. For example, Yagi-Uda antennas operate in the VHF and UHF bands, and one of the most common usages is the receiving of the television broadcasts [7]. However, because of their high directivity and focused radiation beam dish antennas are actively used in satellite systems and deep space studies [8]. Horn antennas are also another type of directional antennas and work in the UHF band [9]. Horn antennas are preferred especially in radar systems. Besides all these antenna types, due to their small volume, two-dimensional structure, and high-performance patch antennas are used in platforms where physical limitations exist such as spacecraft, mobile devices, satellites, and missiles [10, 11]. Since patch antennas are easy-to-produce, inexpensive, and have high price-performance ratio due to their simple structures, their popularities are growing day by day [12].

A traditional patch antenna consists of 3 layers. There is a metallic radiator patch on the upper surface, the ground plane on the bottom layer, and a dielectric substrate sandwiched between them. The characteristics of the antenna are mainly determined by the substrate material and the shape of the metallic radiator patch. In literature various antennas with very different radiator patch geometries such as rectangular and circular shaped [13, 14], triangular shaped [15], and U-shaped patch antennas are reported [16]. These antennas have a few geometrical parameters that allow to set operating frequency. Another type of patch antenna investigated in literature is comb-shaped patch antenna [17, 18]. Unlike the above mentioned antennas, comb-shaped patch antennas have more geometrical parameters useful for setting antenna parameters. However, in all these works antenna geometries are designated to be symmetrical which results in symmetric far-field pattern and radiation. As far as we know there is no study in literature that introduces patch antennas with asymmetric geometry designed in a controlled way and investigates changes of antenna performance and parameters.

In this study, we designed comb-shaped patch antennas with two and three arms at each side evolved from conventional rectangular patch antenna resonating at 5 GHz and investigated changes of the antenna behavior as the symmetrical geometry of the antenna is disrupted by shifting arms on one side of the antenna in a controlled way. With full set of simulations, the changes in the antenna parameters that are resonance frequency, directivity, half power beam width, and side lobe level by shifting the arms were examined. Results show that the proposed asymmetrical geometry of the antenna enables the radiation to occur at a desired angle with a specific side lobe level. It means, instead of adding a third dimension to the antenna, one can

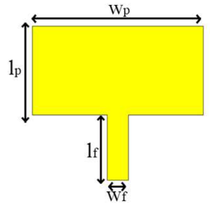

Fig. 1. Designed rectangular patch antenna geometry and its parameters.

adjust the far-field pattern of the antenna in the desired direction by shifting the arms and forming asymmetrical structure on the two-dimensional (2D) comb-shaped patch antenna, which is useful especially for applications in a limited area and volume. In addition, simulation results indicate that for the studied comb-shaped antennas the resonance frequency and directivity of the antenna can be arranged with arm shift in a controlled manner.

II. Antenna Designs

As a first step, a rectangular patch antenna was designed to operate at 5 GHz. The substrate material of the antenna was chosen FR-4 and is sandwiched between two copper layers in the designed antenna. The thickness of the substrate material and the two copper layers in the designed antennas were set to be 1.59 mm and 0.035mm, respectively. Geometry of the designed rectangular patch antenna is shown in Fig. 1. The width (w_p) and length (l_p) of the radiator patch in the designed antenna are 26.25 mm and 13.56 mm, respectively. These values were found with optimization in the simulation tool for the antenna to operate at 5 GHz frequency. To set the input impedance to 50 ohms, on the other hand, the width of the feeding line (w_f) was adjusted to be 3.31 mm and its length (l_f) was set 10 mm.

Next, comb-shaped antenna with arms on its both sides was designed. To this end, some portions of the radiator patch in the rectangular antenna have been removed. The created comb-shaped antenna was primarily designed with two arms on both sides, which is shown in Fig. 2(a). As seen in the figure the antenna has symmetric architecture with consecutive arms on each side having a constant width (w) separated from each other by a uniform spacing (d). The width and distance between the arms are related with each other such that the total width of the radiating patch is the same with the length of the designed rectangular patch antenna that equals to 13.56 mm. Also, arm lengths of the designed comb-shaped antennas are set constant to be equal to half of the difference between the width of the designed rectangular antenna and width of the feeding line, i.e. 11.47 mm ((26.25 mm – 3.31 mm) / 2).

Later, arms on one side (here it is left) of the designed comb-shaped antenna were shifted towards the feeding point. By this way, symmetrical geometry of the antenna is transformed into asymmetrical geometry. The radiation occurs from the designed symmetric comb-shaped antenna with two equal main beams positioned symmetrically with respect to the opposite, i.e., broadside, direction of the antenna. However, by shifting the arms and converting the antenna geometry to be asymmetric it is aimed to strengthen one of the main beams radiated from the comb-shaped antenna while weakening the other. The comb-shaped antenna having two arms on both sides shifted with respect to each other is shown in Fig. 2(b). In the figure shifting distance of the arms on left side with respect to the arms on right is labelled as s.

After, analysis were repeated with comb-shaped antenna having three arms on both sides. As in the comb-shaped antenna with two arms, the comb-shaped antenna having three arms on both sides was first designed to have a symmetric architecture. The geometry of the comb-shaped antenna with three-arms on both sides and its parameters are represented in Fig. 3(a). As seen, the distance between the consecutive arms on one side (d) is fixed. Also, the arm widths (w) are equal to each other. The arm lengths, on the other hand, are constant and equal to the length of the arms in the double arm comb-shaped antenna.

Lastly, as with the comb-shaped antenna having 2 arms on each side, the arms on one side of the designed comb-shaped antenna with three arms on its sides were shifted towards the feeding line. By this way, again the antenna symmetry is disrupted and it is aimed to strengthen one of the main beams radiated from the comb-shaped antenna and increase directivity together with adjusting side lobe level while rotating the main radiation beam to a desired direction. The comb-shaped antenna geometry with three arms on both sides shifted with respect to each other is shown in Fig. 3(b). As in Fig. 2(b), here shifting of the arms on the left side with respect to the arms on the right side is marked with s.

III. Results And Discussion

Simulations were started with the designed rectangular patch antenna (see Fig. 1) with radiator patch sizes equal to 26.25 mm and 13.56 mm. S11 parameter change of the antenna with frequency calculated in simulations over the range spanning from 0 to 10 GHz is shown in Fig. 4. As expected, in the figure it is seen that the antenna resonates at 5 GHz frequency with S11 parameter magnitude equals to -55 dB at the resonance. In the simulations, 3D radiation pattern of the antenna in far-field was calculated, too. The far-field radiation (here directivity) pattern of the antenna at 5 GHz resonance frequency found in the simulations is shown in Fig. 5. It is seen that the radiation pattern is symmetric with respect to the direction opposite of the antenna. Also, there is a single lobe with a maximum directivity value of 6.905 dBi in the broadside direction of the antenna and the half power

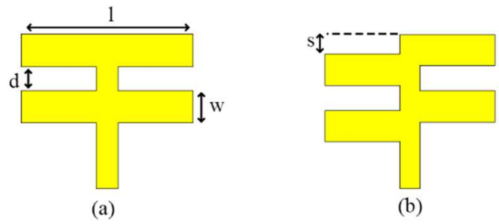

Fig 2. Comb-shaped antenna with two arms on both sides and the geometrical parameters. (a) Symmetric comb geometry with no shift between the arms, (b) asymmetric comb geometry with a shift between the arms on the left and right sides.

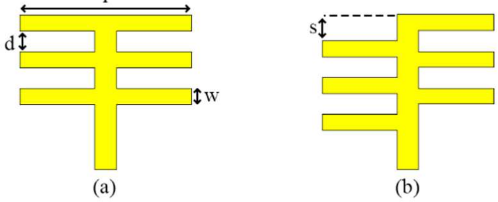

Fig. 3. Comb-shaped antenna with three arms on both sides and the geometrical parameters. (a) Symmetric comb geometry with no shift between the arms, (b) asymmetric comb geometry with a shift between the arms on the left and right sides.

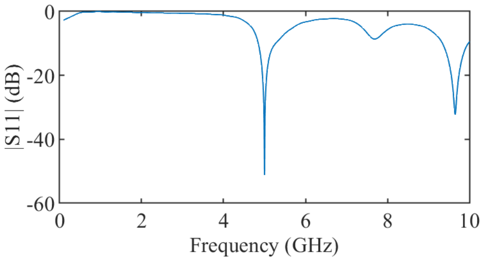

Fig. 4. S11 parameter magnitude change of the designed rectangular antenna with frequency calculated in simulations.

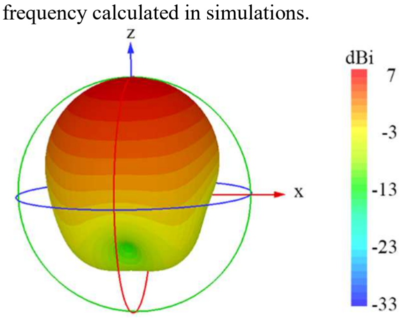

Fig. 5. Far-field directivity pattern of the antenna at 5 GHz resonance frequency calculated in simulations.

beamwidth is 78.9°.

Next, simulations were performed for the designed comb-shaped antenna with two arms on both sides. As explained before, the length and width of the arms in the designed antenna equal to 11.47 mm and 5 mm, respectively. Also, distance between the consecutive arms on one side is set to 3.56 mm. The total width of the radiator patch is 26.25 mm same with the rectangular patch antenna. The simulations were first obtained for the antenna with symmetric geometry and then repeated for the asymmetric geometry with different arm shifts from 0 mm till 9.8 mm with 0.2 mm interval. S11 magnitude change of the antennas calculated in simulations is shown in Fig. 6. In the figure, for clear illustration results obtained for arm shifts that are integer values between 0 mm and 9 mm are presented.

As seen, two resonances occur around 2.75 GHz and 5.2 GHz, respectively. In addition, a third resonance arises in some cases around 8.55 GHz but it is not investigated deeply since it only occurs for a few cases. In the figure, it is also seen that both the first and second resonances shift to lower frequencies as the arm shifting increases. On the other hand, the first resonance around 2.75 GHz gets stronger while the second resonance around 5.2 GHz diminishes as the arm shift increases. Changes of the first and second resonance frequencies with arm shift are shown in Fig 7(a) and (b), respectively. In subfigure 7(a) the markers start from the 4.2 mm shifting because S11 parameter magnitudes of the antennas with arm shift lower than 4.2 mm are above -10 dB at the first resonances. However, in the subfigure it is also seen that the first resonance frequency of the antenna decreases almost linearly with shifting until the shifting equals to 9.4 mm. This is an important observation indicating that the first resonance of the designed comb-shaped antenna can be decreased to lower frequencies by simply shifting the arms on one side without enhancing the total area of the radiator patch. However, after 9.4 mm shifting the first resonance frequency stays almost constant. On the other hand, in subfigure 7(b) the data start from 0 mm shifting and it is observed that the resonance frequency is 5.45 GHz for the case of 0 mm shifting. However, in the subfigure it is

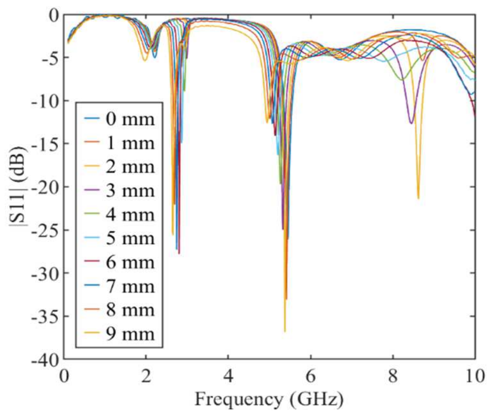

Fig. 6. S11 parameter magnitude change of the designed comb-shaped antenna having two arms on both sides with frequency calculated in simulations for various shifting distances.

also observed that the resonance frequency decreases as the shifting of the arms increases. This is a continuous decrease and persists up to 4.9 GHz at 9.9 mm shifting in the figure.

After S11 parameter and resonance frequency analysis, the far-field directivity patterns of the designed comb-shaped antenna with two arms on both sides at resonance frequencies around 5.2 GHz were calculated, too. Since resonance frequency alters with arm shift, simulations were repeated for each arm shift case at corresponding resonance frequency. In Fig. 8 3D far-field directivity patterns of the antenna for three different arm shifting distances at corresponding resonance frequencies are shown. As seen in the figure, the radiation occurs with two symmetric main beams for 0 mm shifting. It is expected because 0 mm shifting corresponds to comb-shaped antenna with symmetric geometry. However, as the arms slide the beam on the side of the shifted arms gets stronger while the beam on the other side gets weaker. It is seen that as the shifting increases the maximum directivity achieved by the antenna increases, too. Also, the side lobe level of the antenna decreases with arm shifting. Change of the maximum directivity achieved by the

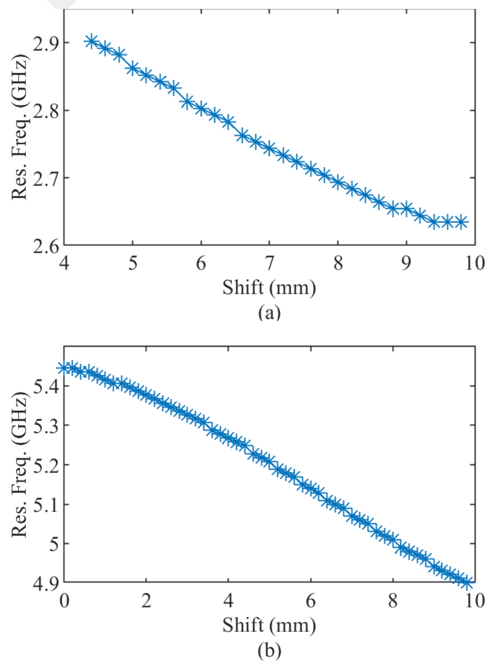

Fig. 7. Resonance frequency change of the designed comb-shaped antenna having two arms on both sides with arm shifting. (a) The first resonance around 2.75 GHz, (b) the second resonance around 5.2 GHz.

antenna with arm shift at corresponding resonance frequencies around 5.2 GHz is shown in Fig. 9. Also, the side lobe level change of the antenna with arm shift is shown in Fig. 10. In Fig. 9 it is seen that directivity of the designed comb-shaped antenna having two arms on both sides increases with arm shift, such that it increases from 6.2 dBi to 7.6 dBi for 0 mm and 8 mm arm shift values, respectively. However, speed of the increase gets slower as the arms shift more and at 9 mm arm shift the directivity value decreases to 7.5 dBi. In Fig. 10, on the other hand, continuous decrease in side lobe level is seen. The side lobe level of the designed antenna decreases from 0 dB to -7 dB as the arms shift from 0 mm to 9 mm.

In addition to the directivity and side lobe level, half power beam width of the antenna varies as the arms are shifted in the designed comb-shaped antenna. Change of the half power beam width of the designed antenna with arm shift calculated at corresponding resonance frequencies around 5.2 GHz is shown in Fig. 11. In the figure it is seen that the half power beam width increases continuously with arm shifting. The half power beam width of the antenna is found 55.6° in the case of no shift between the arms and it increases up to 61.2° when 9 mm arm shift is applied.

After comb-shaped antenna analysis with two arms on both sides, simulations were repeated for the comb-shaped antenna design having three arms on both sides. As in the comb-shaped antenna with two arms on the sides, the length

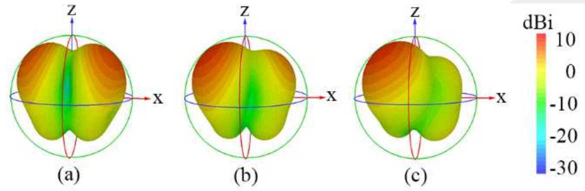

Fig. 8. 3D far-field directivity pattern of the antenna for (a) 0 mm arm shifting, (b) 5 mm arm shifting, (c) 9 mm arm shifting, calculated at resonance frequency of 5.446 GHz, 5.208 GHz, and 4.941 GHz, respectively.

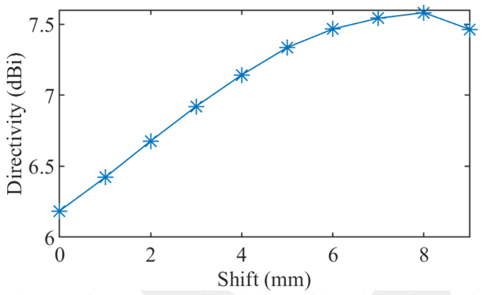

Fig. 9. Change of maximum directivity achieved by the designed comb-shaped antenna having two arms on both sides with arm shift calculated at corresponding resonance frequencies around 5.2 GHz.

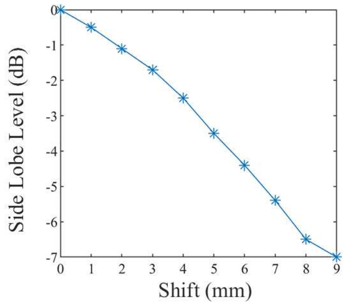

Fig. 10. Side lobe level change of the designed comb-shaped antenna having two arms on both sides with arm shift calculated at corresponding resonance frequencies around 5.2 GHz.

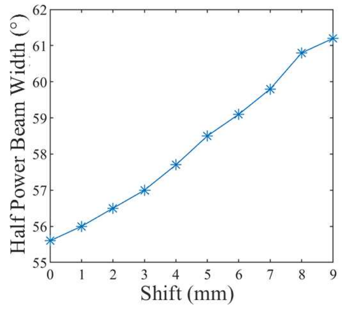

Fig. 11. Half power beam width change of the designed comb-shaped antenna having two arms on both sides with arm shift calculated at corresponding resonance frequencies around 5.2 GHz.

and width of the arms in the designed antenna equal to 11.47 mm and 5 mm, respectively. In addition, for fair comparison, total width of the radiator patch is set to be 26.25 mm same with that of the designed rectangular antenna and comb-shaped antenna with two arms. The simulations were again first performed for the designed antenna with no shift between the arms on the sides and then for the antenna with various shifting distances. S11 magnitude change of the designed comb-shaped antenna with three arms on both sides having symmetrical and asymmetrical geometries calculated in simulations is shown in Fig. 12. In the figure it is seen that two resonances occur around 2.9 GHz and 5.2 GHz. Also, a third resonance arises around 8.95 GHz. This is the same with the behavior observed for the designed comb-shaped antenna with two arms on the sides. Since the third resonance around 8.95 GHz appears strong enough, i.e., below -10 dB, only for few cases, here again only the first two resonances are investigated. In the figure it is seen that both the first and second resonances shift to lower frequencies as the arm shifting increases. On the other hand, the first resonance has a tendency to be stronger with the arm shift, whereas the second resonance has a tendency to weaken as the arm shift enhances. Changes of the first and second resonance frequencies of the designed antenna having three arms on the sides with arm shift are illustrated in Fig. 13.

In the figure it is seen that the designed comb-shaped antenna with three arms on its sides having a symmetrical geometry resonates at 3.12 GHz and 5.49 GHz. Both of the resonance frequencies decrease with arm shifting such that the first resonance frequency decreases to 2.71 GHz and the second resonance frequency decreases to 4.91 GHz when the arms on one side are shifted by 10 mm with respect to the arms on the other side. In subfigure (a) it is clear that the first resonance frequency decreases continuously till 9.3 mm and

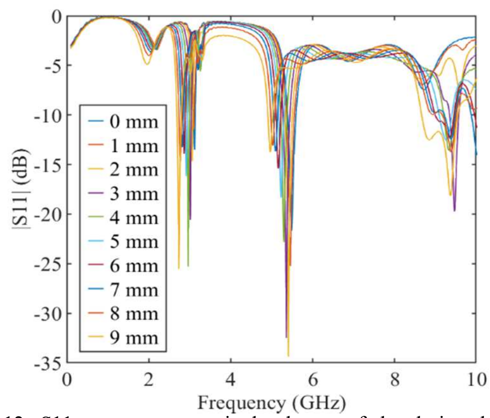

Fig. 12. S11 parameter magnitude change of the designed comb-shaped antenna having three arms on both sides with frequency calculated in simulations for various shifting distances.

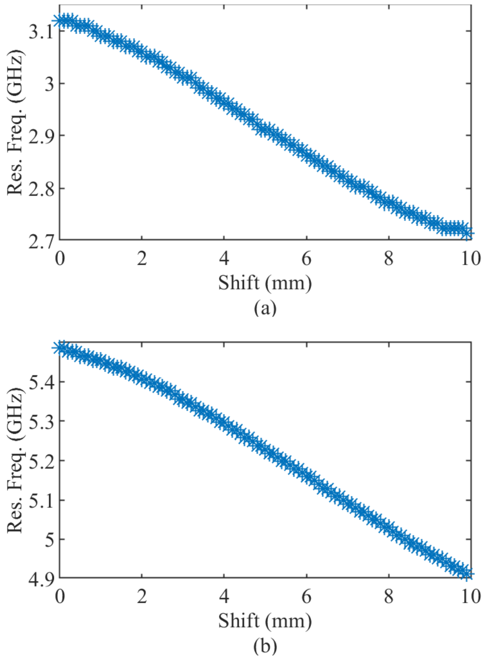

Fig. 13. Resonance frequency change of the designed comb-shaped antenna having three arms on both sides with arm shifting. (a) The first resonance around 2.9 GHz, (b) the second resonance around 5.2 GHz.

after 9.3 mm arm shift the resonance frequency stays almost constant. On the other hand, in subfigure (b) it is seen that the second resonance frequency of the designed comb-shaped antenna having three arms on both sides decreases monotonically with the arm shift for the arm shifting distances between 0 mm and 10 mm. These observations are the same with that obtained for the designed comb-shaped antenna having two arms on the sides. For further investigation, the far-field directivity pattern of the designed antenna with three-arms on the sides was calculated, too. In Fig. 14 far-field patterns of the designed antenna for three different arm shift distances calculated at resonance frequencies around 5.2 GHz are shown. As seen in the figure, radiation occurs with two equal and symmetrical main beams for the antenna having no shift between the arms. This is the same with what was observed before for the antenna with two arms on the sides. However, as the arm shifting increases the beam on the side of the arms closer to the feeding line gets stronger, whereas the other beam on the side of the arms further away from the feeding line diminishes. Change of the maximum directivity achieved by the designed antenna at corresponding resonance frequencies around 5.2 GHz with arm shifting is shown in Fig. 15. In addition, side lobe level change of the designed antenna with arm shifting is shown in Fig. 16.

In Fig. 15 it is seen that the directivity of the designed antenna having three arms on both sides has an increasing trend with arm shift such that the directivity increases from 6.2 dBi to 7.7 dBi as the arm shifting is applied starting from 0 mm till 8 mm. After 8 mm arm shifting the directivity decreases slowly. This is the same with what was observed before for the designed comb-shaped antenna having two arms on the sides. In Fig. 16, on the other hand, it is seen that the side lobe level of the designed comb-shaped antenna having three arms on both sides decreases continuously with arm shifting. The side lobe level decreases from 0 dB to -7.2 dB as the arm shift extends from 0 mm to 9.5 mm. Moreover, half power beam width variation of the designed antenna with three arms on the sides were examined, too. As

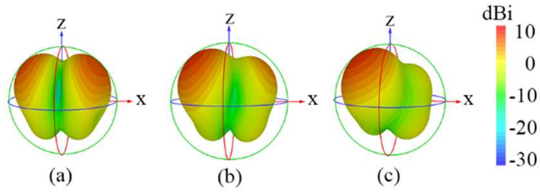

Fig. 14. 3D far-field directivity pattern of the antenna for (a) 0 mm arm shifting, (b) 5 mm arm shifting, (c) 9.5 mm arm shifting, calculated at resonance frequency of 5.486 GHz, 5.228 GHz, and 4.931 GHz, respectively.

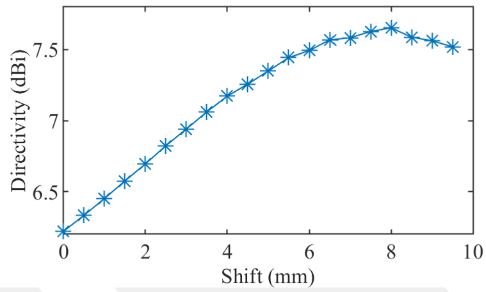

Fig. 15. Change of maximum directivity achieved by the designed comb-shaped antenna having three arms on both sides with arm shift calculated at corresponding resonance frequencies around 5.2 GHz.

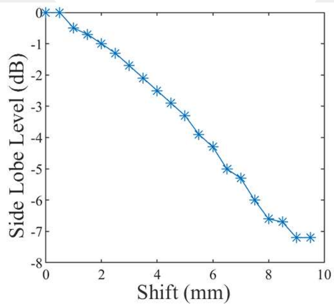

Fig. 16. Side lobe level change of the designed comb-shaped antenna having three arms on both sides with arm shift calculated at corresponding resonance frequencies around 5.2 GHz.

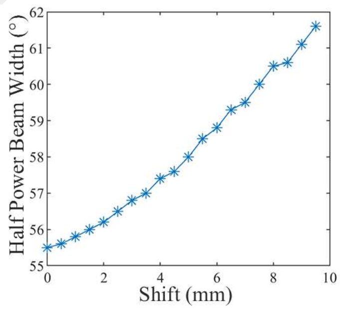

Fig. 17. Half power beam width change of the designed comb-shaped antenna having three arms on both sides with arm shift calculated at corresponding resonance frequencies around 5.2 GHz.

seen in Fig. 14, radiation and beam width of the antenna alter depending on the arm shift. Half power beam width change of the designed comb-shaped antenna having three arms on both sides with arm shift calculated at resonance frequencies around 5.2 GHz is shown in Fig. 17. In the figure it is seen that the half power beam width of the antenna is 55.5° for 0 mm arm shifting and it increases with arm shift to 61.6° in the case of 9.5 mm arm shifting. Results show that both the designed antennas having two and three arms on the sides exhibit very similar behaviors with arm shifts. For further comparisons, the simulations were obtained for the same antennas with different arm thicknesses. The same observations were held with that reported in the paper.

IV. Conclusion

In this study, comb-shaped patch antennas having two and three arms at the sides with symmetrical and asymmetrical geometries are investigated. The designed symmetrical comb-shaped antenna is evolved from a regular rectangular shaped antenna and the asymmetrical comb-shaped antenna geometry is obtained by shifting the arms on one side of the symmetrical antenna. The designed symmetrical and asymmetrical antennas were analyzed with 3D simulations for various arm shifting distances. Results show that the designed antenna characteristics of resonance frequency and radiation pattern alter in controlled manner as the arms on one side of the antenna shift.

In the simulations, it is observed that the comb-shaped antennas perform more than two resonances. The first resonance frequencies of the designed antennas decrease with arm shift till a certain arm shifting distance, whereas the second resonance frequencies of the antennas decrease continuously with arm shifting. It indicates that the resonance frequencies of the comb-shaped antennas can be set to lower frequencies by simply shifting the arms on one side of the antennas without changing the total radiation patch area.

In addition, in simulations it is seen that radiation occurs in the designed comb-shaped antennas at the second resonance frequency with two beams. In symmetric geometry where no shift is applied to the arms, two main beams with equal intensities arise symmetrically with respect to the broadside direction. When shifting is applied the main beam on the side of the arms closer to the feeding line gets stronger, whereas the other beam on the side of the arms away from the feeding line weakens. Calculated results show that the maximum directivities of the designed comb-shaped antennas have a tendency to increase with the arm shifting. As the arms on one side of the antennas are shifted the maximum directivities achieved by the antennas increase. However, speed of the increase gets slower as the arms shift more and after a specific arm shifting distance the directivity value of a designed antenna decreases. Moreover, in the simulations it is observed that side lobe level of the designed comb-shaped antennas continuously decreases with the arm shift. It is an expected result because as the arms on one side of the antennas are shifted the main beam becomes stronger while the side lobe gets weaker. The half power beam width of the designed antennas, on the other hand, increases with arm shift.

The findings of this study demonstrate that with the proposed asymmetrical comb-shaped antenna geometry it is possible to shift the resonance frequency, adjust the radiation pattern and change the radiation characteristics of directivity, side lobe level, and half power width in a controlled way without need to make the antenna design 3D, which is beneficial for applications with limited size requirements including satellite and mobile communication systems, and RFID and Internet of Things (IoT) applications.

References

[1] *C.A. Balanis, Antenna Theory Analysis and Design, 4th ed. Hoboken, NJ: Wiley, 2016, pp. 783-867.*

[2] A. Q. Khan, M. Riaz, and A. Bilal, “Various Types of Antenna with Respect to their Applications: A Review,” *International Journal of Multidisciplinary Sciences and Engineering*, vol. 7, no. 3, pp. 1–8, Mar. 2016.

[3] A. T. Mobashsher and A. M. Abbosh, “*Performance of directional and omnidirectional antennas in wideband head imaging,” IEEE Antennas and Wireless Propagation Letters,* vol. 15, pp. 1618–1621, 2016, doi: 10.1109/LAWP.2016.2519527.

[4] M. J. Salter, “The design of dipole and monopole antennas with low uncertainties,” *IEEE Transactions on Instrumentation and Measurement*, vol. 46, no. 2, pp. 539–543, Apr. 1997, doi: 10.1109/19.571905.

[5] T. S. Rappaport, G. R. MacCartney, S. Sun, H. Yan, and S. Deng, “Small-Scale, Local Area, and Transitional Millimeter Wave Propagation for 5G Communications,” *IEEE Transactions on Antennas and Propagation*, vol. 65, no. 12, pp. 6474–6490, Dec. 2017, doi: 10.1109/TAP.2017.2734159.

[6] L. Ithayakumaran, “Antennas and its Applications,” *Academia*, pp. 66–78, Mar. 2009.

[7] P. V. Nikitin and K. V. S. Rao, “Compact Yagi antenna for handheld UHF RFID reader,” in *2010 IEEE Antennas and Propagation Society International Symposium*, Jul. 2010, pp. 1–4. doi: 10.1109/APS.2010.5562224.

[8] J. Gaspar *et al.*, “Test and Analysis of an Inflatable Parabolic Dish Antenna,” in *47th AIAA/ASME/ASCE/AHS/ASC Structures, Structural Dynamics, and Materials Conference*, American Institute of Aeronautics and Astronautics. doi: 10.2514/6.2006-1600.

[9] L. Peiguo, L. Kecheng, H. Jianguo, Y. Jiaxian, Z. Guangfu, and M. Junjie, “Analysis of a ultra-wide band planar horn antenna for UHF,” in *1999 International Conference on Computational Electromagnetics and its Applications. Proceedings (ICCEA’99) (IEEE Cat. No.99EX374)*, Nov. 1999, pp. 226–228. doi: 10.1109/ICCEA.1999.825111.

[10] Z. Li, K. Wu, and T. A. Denidni, “A new approach to integrated horn antenna,” in *2004 10th International Symposium on Antenna Technology and Applied Electromagnetics and URSI Conference*, Jul. 2004, pp. 1–3. doi: 10.1109/ANTEM.2004.7860646.

[11] N. Supreeyatitikul, T. Lertwiriyaprapa and C. Phongcharoenpanich, "S-Shaped Metasurface-Based Wideband Circularly Polarized Patch Antenna for C-Band Applications," in IEEE Access, vol. 9, pp. 23944-23955, 2021, doi: 10.1109/ACCESS.2021.3056485.

[12] I. Singh and V. S. Tripathi, “Micro strip Patch Antenna and its Applications: a Survey,” *International Journal of Computer Technology and Applications*, vol. 2, no. 5, pp. 1595–1599, Sep. 2011.

[13] H. Werfelli, K. Tayari, M. Chaoui, M. Lahiani, and H. Ghariani, “Design of rectangular microstrip patch antenna,” in *2016 2nd International Conference on Advanced Technologies for Signal and Image Processing (ATSIP)*, Mar. 2016, pp. 798–803. doi: 10.1109/ATSIP.2016.7523197.

[14] K. M. Mak, H. W. Lai, K. M. Luk, and K. L. Ho, “Polarization Reconfigurable Circular Patch Antenna With a C-Shaped,” *IEEE Transactions on Antennas and Propagation*, vol. 65, no. 3, pp. 1388–1392, Mar. 2017, doi: 10.1109/TAP.2016.2640141.

[15] J. Row and Y. Liou, “Broadband short-circuited triangular patch antenna,” IEEE Transactions on Antennas and Propagation, vol. 54, no. 7, pp. 2137–2141, Jul. 2006, doi: 10.1109/TAP.2006.875916.

[16] S. Kannadhasan and A. C. Shagar, “Design and analysis of U-shaped micro strip patch antenna,” in 2017 Third International Conference on Advances in Electrical, Electronics, Information, Communication and Bio-Informatics (AEEICB), Feb. 2017, pp. 367–370. doi: 10.1109/AEEICB.2017.7972333.

[17] H. Baydar, M. Aslan, and V. T. Kilic, “Single and Double Side Comb-Shaped Patch Antenna Design Evolved from Rectangular Shape for Reduced Sized Antenna Applications,” in 2020 International Conference on Radar, Antenna, Microwave, Electronics, and Telecommunications (ICRAMET), Nov. 2020, pp. 28–33. doi: 10.1109/ICRAMET51080.2020.9298603.

[18] E. Marongiu et al., "Design and Characterization of Modified Comb Patch Antennas," in IEEE Access, vol. 10, pp. 36220-36232, 2022, doi: 10.1109/ACCESS.2022.3164072.